

The motion of stars near the Galactic center: A comparison of the black hole and fermion ball scenarios

Faustin Munyaneza and Raoul D. Viollier

Institute of Theoretical Physics and Astrophysics

Department of Physics, University of Cape Town

Private Bag, Rondebosch 7701, South Africa

fmunyaneza@hotmail.com, viollier@physci.uct.ac.za

Received _____; accepted _____

ABSTRACT

After a discussion of the properties of degenerate fermion balls, we analyze the orbits of the stars S0-1 and S0-2, which have the smallest projected distances to Sgr A*, in the supermassive black hole as well as in the fermion ball scenarios of the Galactic center. It is shown that both scenarios are consistent with the data, as measured during the last six years by Genzel et al. and Ghez et al. The free parameters of the projected orbit of a star are the unknown components of its velocity v_z and distance z to Sgr A* in 1995.4, with the z -axis being in the line of sight. We show, in the case of S0-1 and S0-2, that the $z - v_z$ phase-space, which fits the data, is much larger for the fermion ball than for the black hole scenario. Future measurements of the positions or radial velocities of S0-1 and S0-2 could reduce this allowed phase-space and eventually rule out one of the currently acceptable scenarios. This may shed some light into the nature of the supermassive compact dark object, or dark matter in general at the center of our Galaxy.

Subject headings: black hole physics-celestial mechanics, stellar dynamics dark matter - elementary particles - Galaxy: center

1. Introduction

There is strong evidence for the existence of a supermassive compact dark object near the enigmatic radio source Sagittarius A* (Sgr A*) which is located at or close to the dynamical center of the Galaxy (Rogers et al. 1994; Genzel et al. 1997; Lo et al. 1998; Ghez et al. 1998). Stars observed in the $2.2\ \mu\text{m}$ infrared K-band at projected distances $\gtrsim 5$ mpc from Sgr A*, and moving with projected velocities $\lesssim 1400\ \text{km s}^{-1}$, indicate that a mass of $(2.6 \pm 0.2) \times 10^6 M_\odot$ must be concentrated within a radius ~ 15 mpc from Sgr A* (Haller et al. 1996; Eckart and Genzel 1996, 1997; Genzel & Townes 1987; Genzel et al. 1994, 1996, 1999, 2000; Ghez et al. 1998, 2000). VLBA radio interferometry measurements at 7 mm wavelength constrain the size of the radio wave emitting region of Sgr A* to $\lesssim 1$ AU in E-W direction and ~ 3.6 AU in N-S direction (Rogers et al. 1994, Bower and Backer 1998, Krichbaum et al. 1994, Lo et al. 1998), and the proper motion of Sgr A* relative to the quasar background to $\lesssim 20\ \text{km s}^{-1}$ (Baker 1996; Reid et al. 1999; Baker and Sramek 1999). As the fast moving stars of the central cluster interact gravitationally with Sgr A*, the proper motion of the radio source cannot remain as small as it is now for ~ 200 kyr unless Sgr A* is attached to some mass $\gtrsim 10^3 M_\odot$. In spite of these well-known stringent facts, the enigmatic radio source Sgr A*, as well as the supermassive compact dark object that is perhaps associated with it, are still two of the most challenging mysteries of modern astrophysics.

It is currently believed that the enigmatic radio source Sgr A* coincides in position with a supermassive black hole (BH) of $(2.6 \pm 0.2) \times 10^6 M_\odot$ at the dynamical center of the Galaxy. Although standard thin accretion disk theory fails to explain the peculiar low luminosity $\lesssim 10^{37}\ \text{erg s}^{-1}$ of the Galactic center (Goldwurm et al. 1994), many models have been developed that describe the spectrum of Sgr A* fairly well, based on the assumption that it is a BH. The models proposed for the radio emission, range from quasi-spherical

inflows (Melia 1994; Narayan and Mahadevan 1995; Narayan et al. 1998; Mahadevan 1998) to a jet-like outflow (Falcke, Mannheim and Biermann 1993; Falcke and Biermann 1996; Falcke and Biermann 1999). Yet, as some of these models appear to contradict each other, not all of them can represent the whole truth. We also note that the Galactic center is a weak source of diffuse emission in the 2-10 keV energy range and in the lines of several ions (Sunyaev et al. 1993; Koyama et al. 1996; Sidoli and Mereghetti 1999). Thus, apart from earthbound VLBA radio interferometers, space missions such as the European Multi-Mirror satellite (XMM) and Chandra X-ray satellite, may eventually provide conclusive evidence for the nature of Sgr A* and the supermassive compact dark object at the Galactic center. In fact, the Chandra X-ray satellite has recently detected a point source at the location of Sgr A* (Baganoff et al. 1999) with a luminosity two times smaller than the upper limit set by the ROSAT satellite some years ago (Predehl and Trümper 1994). For more detailed recent reviews on the Galactic center we refer to Morris and Serabyn 1996, Genzel and Eckart 1999, Kormendy and Ho 2000, and Yusef-Zadeh et al. 2000.

Supermassive compact dark objects have also been inferred at the centers of many other galaxies, such as M87 (Ford et al. 1994; Harms et al. 1994; Macchetto et al. 1997) and NGC 4258 (Greenhill et al. 1995; Myoshi et al. 1995). For recent reviews we refer to Richstone et al. 1998, Ho and Kormendy 2000, and Kormendy 2000. In fact, perhaps with the exception of dwarf galaxies, all galaxies may harbor such supermassive compact dark objects at their centers. However, only a small fraction of these show strong radio emission similar to that of the enigmatic radio source Sgr A* at the center of our Galaxy. For instance M31 does not have such a strong compact radio source, although the supermassive compact dark object at the center of M31 has a much larger mass ($\sim 3 \times 10^7 M_\odot$) than that of our Galaxy (Dressler and Richstone 1988; Kormendy 1988). It seems, therefore, prudent not to take for granted that the enigmatic radio source Sgr A* and the supermassive compact dark object at the center of our Galaxy are necessarily one and the same object.

An unambiguous proof for the existence of a BH requires the observation of stars moving at relativistic velocities near the event horizon. However, in the case of our Galaxy, the stars S0-1 and S0-2, that are presumably closest to the suspected BH, reach projected velocities $\lesssim 1400$ km s $^{-1}$. Assuming a radial velocity of $v_z = 0$, this corresponds to the escape velocity at a distance $\gtrsim 5 \times 10^4$ Schwarzschild radii from the BH. Thus any dark object, having a mass $\sim 2.6 \times 10^6 M_\odot$ and a radius $\lesssim 5 \times 10^4$ Schwarzschild radii, would fit the current data on the proper motion of the stars of the central cluster as well as the BH scenario. One of the reasons why the BH scenario of Sgr A* is so popular, is that the only baryonic alternative to a BH that we can imagine, is a cluster of dark stars (e.g. brown dwarfs, old white dwarfs, neutron stars, etc.), having a total mass of $\sim 2.6 \times 10^6 M_\odot$ concentrated within a radius of ~ 15 mpc. However, such a star cluster would disintegrate through gravitational ejection of stars on a time scale $\lesssim 100$ Myr, which is much too short to explain why this object still seems to be around today ~ 10 Gyr after its likely formation together with the Galaxy (Sanders 1992; Haller et al. 1996; Maoz 1995, 1998). Nevertheless, in order to test the validity of the BH hypothesis meaningfully, we definitely need an alternative and consistent finite size model of the supermassive compact dark objects at the galactic centers.

2. The case for degenerate fermion balls

It is well known that our Galactic halo is dominated by dark matter, the bulk part of which must be nonbaryonic (Alcock 2000). Numerical simulations show that dark matter in the form of a gas of weakly interacting massive particles, will eventually produce a high-density spike at the center of the Galaxy (Navarro et al. 1997; Gondolo & Silk 1999). It is therefore conceivable that the supermassive compact dark object at the center of our Galaxy is made of the same dark matter that dominates the Galactic halo at large. In fact,

some years ago, we suggested that the supermassive compact dark object at the Galactic center may be a gravitationally stable ball of weakly interacting fermions in which the degeneracy pressure balances the gravitational attraction of the massive fermions (Viollier et al. 1992, 1993; Viollier 1994; Tsiklauri & Viollier 1996; Bilić, Munyaneza & Viollier 1999). Such degenerate fermion balls (FBs) could have been formed in the early universe during a first-order gravitational phase transition (Bilić & Viollier 1997, 1998, 1999a,b). A further formation mechanism of FBs that is based on gravitational ejection of degenerate matter has recently been discussed in Bilić et al. 2000.

There are three main reasons why it is worthwhile to study such degenerate FBs as an alternative to BHs at the center of the galaxies, in particular our own:

- (i) Introducing a weakly interacting fermion in the $\sim 13 \text{ keV}/c^2$ to $\sim 17 \text{ keV}/c^2$ mass range, one can explain the full range of the masses and radii of the supermassive compact dark objects, that have been observed so far at the galactic centers, in terms of degenerate FBs with masses ranging from 10^6 to $10^{9.5} M_\odot$ (Kormendy and Richstone 1995; Richstone et al. 1998). The maximal mass allowed for a FB composed of degenerate fermions of a given mass m_f and degeneracy factor g_f is the Oppenheimer-Volkoff (OV) limit $M_{OV} = 0.54195 M_{Pl}^3 m_f^{-2} g_f^{-\frac{1}{2}} = 2.7821 \times 10^9 M_\odot$ $(15 \text{ keV}/m_f c^2)^2 (2/g_f)^{\frac{1}{2}}$, where $M_{Pl} = (\hbar c/G)^{\frac{1}{2}}$ is the Planck mass (Bilić, Munyaneza & Viollier 1999). It is tempting to identify the mass of the most massive compact dark object ever observed at a center of a galaxy (Kormendy & Ho 2000), e.g. that of the center of M87, with the OV-limit, i.e. $M_{OV} = (3.2 \pm 0.9) \times 10^9 M_\odot$ (Macchetto et al. 1997). This requires a fermion mass of $12.4 \text{ keV}/c^2 \lesssim m_f \lesssim 16.5 \text{ keV}/c^2$ for $g_f = 2$, or $10.4 \text{ keV}/c^2 \lesssim m_f \lesssim 13.9 \text{ keV}/c^2$ for $g_f = 4$. For $M_{OV} = 3.2 \times 10^9 M_\odot$ such a relativistic FB would have a radius of $R_{OV} = 4.45 R_{OV}^s = 1.36 \text{ mpc}$, where R_{OV}^s is the Schwarzschild radius of the mass M_{OV} . It would thus be virtually indistinguishable

from a BH, as the radius of the last stable orbit around a BH is $3 R_{OV}^s = 0.92$ mpc anyway. The situation is quite different for a nonrelativistic FB of mass $M = (2.6 \pm 0.2) \times 10^6 M_\odot$, which for the upper limit of the allowed fermion mass ranges, $m_f = 16.5 \text{ keV}/c^2$ for $g_f = 2$, or $m_f = 13.9 \text{ keV}/c^2$ for $g_f = 4$, would have a radius bound by $16.7 \text{ mpc} \lesssim R \lesssim 17.6 \text{ mpc}$, corresponding to $\sim 7 \times 10^4$ Schwarzschild radii, as the FB radius scales nonrelativistically like $R \propto m_f^{-8/3} g_f^{-2/3} M^{-1/3}$. Such an object is far from being a black hole: its escape velocity from the center is $\sim 1,700 \text{ km s}^{-1}$. As the fermions interact only weakly with the baryons, baryonic stars could also move inside a FB without experiencing noticeable friction with the fermions (Tsiklauri and Viollier 1998a,b; Munyaneza, Tsiklauri and Viollier, 1998, 1999). Since the potential within ~ 10 mpc from the center is rather shallow, star formation in this region will be less inhibited by tidal forces than in the BH case.

- (ii) A FB with mass $M = (2.6 \pm 0.2) \times 10^6 M_\odot$ and radius $R \lesssim 18.4$ mpc is consistent with the current data on the proper motion of the stars in the central cluster around Sgr A*. This implies lower limits for the fermion masses of $m_f \gtrsim 15.9 \text{ keV}/c^2$ for $g_f = 2$ and $m_f \gtrsim 13.4 \text{ keV}/c^2$ for $g_f = 4$, which partly overlap with the fermion mass ranges derived for M87. By increasing the fermion mass, one can interpolate between the FB and the BH scenarios. However, for fermion masses $m_f \gtrsim 16.5 \text{ keV}/c^2$, for $g_f = 2$ and $m_f \gtrsim 13.9 \text{ keV}/c^2$ for $g_f = 4$, the interpretation of some of the most massive compact dark objects in terms of degenerate FBs is no longer possible. It is quite remarkable that we can describe the two extreme cases, the supermassive compact dark object at the center of M87 and that of our Galaxy, in terms of self-gravitating degenerate FBs using a single fermion mass. This surprising fact is a consequence of the equation of state of degenerate fermionic matter; this would not be the case for degenerate bosonic matter. Indeed, for a supermassive object consisting of nonrelativistic self-gravitating degenerate bosons, mass and radius would scale, for a

constant boson mass, as $R \propto M^{-1}$, rather than $R \propto M^{-1/3}$, as for a supermassive object consisting of nonrelativistic self-gravitating degenerate fermions, for a constant fermion mass. The ratio of the radii of the supermassive objects with $10^{6.5} M_\odot$ and $10^{9.5} M_\odot$ would be 10^3 in the boson case, instead of 10 as in the fermion case. Thus it would not be possible to fit mass and radius of both the supermassive compact dark object at the center of M87 and that of our Galaxy, in the boson case. We therefore conclude that, if we want to describe all the supermassive compact dark objects in terms of self-gravitating degenerate particles of the same kind and mass, these objects cannot be composed of bosons, they must consist of fermions.

- (iii) The FB scenario provides a natural cut-off of the emitted radiation at infrared frequencies $\gtrsim 10^{13}$ GHz, as is actually observed in the spectrum of the Galactic center (Bilić, Tsiklauri and Viollier 1998; Tsiklauri and Viollier 1999; Munyaneza and Viollier 1999). This is because matter, e.g. in the form of stars, gas, dust or dark matter, etc. falling from infinity at rest towards the FB, cannot acquire velocities larger than the escape velocity from the center of the FB, i.e. $\sim 1,700$ km s $^{-1}$. Consequently, there is also a natural cut-off of the high-frequency tail of the radiation emitted by the accreted baryonic matter. This is quite a robust prediction of the FB scenario, because it is virtually independent of the details of the accretion model. In a thin disk accretion model, the radiation at the observed cut-off is emitted at distances ~ 10 mpc from the center of the FB. This is also the region, where the gravitational potential becomes nearly harmonic due to the finite size of the FB. The fermion masses required for a cut-off at the observed frequency $\sim 10^{13}$ GHz depend somewhat on the accretion rate and the inclination angle of the disk assumed, but $m_f \lesssim 20$ keV/c 2 for $g_f = 2$ or $m_f \lesssim 17$ keV/c 2 for $g_f = 4$ seem to be reasonable conservative upper limits (Tsiklauri and Viollier 1999, Munyaneza and Viollier 1999).

Summarizing the preceding arguments (i) to (iii), we can constrain the allowed fermion masses for the supermassive compact dark objects in our Galaxy to $15.9 \text{ keV}/c^2 \lesssim m_f \lesssim 16.5 \text{ keV}/c^2$ for $g_f = 2$ or $13.4 \text{ keV}/c^2 \lesssim m_f \lesssim 13.9 \text{ keV}/c^2$ for $g_f = 4$, where the lower limits are determined from the proper motion of stars in the central cluster of our Galaxy, while the upper limits arise from the supermassive compact dark object at the center of M87. This fermion mass range is also consistent with the infrared cut-off of the radiation emitted by the accreted baryonic matter at the Galactic center. Of course, one of the major challenges will be to accommodate, within the FB scenario, the properties of Sgr A* which is perhaps peculiar to our galaxy.

We now would like to identify a suitable candidate for the postulated weakly interacting fermion. This particle should have been either already observed, or its existence should have been at least predicted in recent elementary particle theories. The required fermion cannot be the gaugino-like neutralino, i.e. a linear combination of the bino, wino and the two higgsinos, as its mass is expected to be in the $\sim 30 \text{ GeV}/c^2$ to $\sim 150 \text{ GeV}/c^2$ range (Roszkowski 2001). It cannot be a standard neutrino either (however, see Giudice et al. 2000), as this would violate the cosmological bound on neutrino mass and, more seriously, it would contradict the Superkamiokande data (Fukuda et al. 2000). However, the required fermion could be the sterile neutrino that has been recently suggested as a cold dark matter candidate in the mass range between $\sim 1 \text{ keV}/c^2$ to $\sim 10 \text{ keV}/c^2$ (Shi and Fuller 1999; Chun & Kim 1999; Tupper et al. 2000), although one would have to stretch the mass range a little bit and worry about the (possibly too rapid) radiative decay into a standard neutrino. This sterile neutrino is resonantly produced with a cold spectrum and near closure density, if the initial lepton asymmetry is $\sim 10^{-3}$. Alternatively, it could be either the gravitino, postulated in supergravity theories with a mass in the $\sim 1 \text{ keV}/c^2$ to $\sim 100 \text{ GeV}/c^2$ range (Lyth 1999), or the axino, with a mass in the range between $\sim 10 \text{ keV}/c^2$ and $\sim 100 \text{ keV}/c^2$, as predicted by the supersymmetric extensions of the Peccei-Quinn solution

to the strong CP-problem (Goto & Yamaguchi 1992). In this scenario, the axino mass arises quite naturally as a radiative correction in a model with a no-scale superpotential. In summary, there are at least three promising candidates which have been recently predicted for completely different reasons in elementary particle theories. One of these particles could play the role of the weakly interacting fermion required for the supermassive compact dark objects at the centers of the galaxies and for cold or warm dark matter at large, if its mass is in the range between $\sim 13 \text{ keV}/c^2$ and $\sim 17 \text{ keV}/c^2$ and its contribution to the critical density is $\Omega_f \sim 0.3$.

3. Outline of the paper

The purpose of this paper is to compare the predictions of the BH and FB scenarios of the Galactic center, for the stars with the smallest projected distances to Sgr A*, based on the measurements of their positions during the last six years (Ghez et al. 2000). The projected orbits of three stars, S0-1 (S1), S0-2 (S2) and S0-4 (S4), show deviations from uniform motion on a straight line during the last six years, and they thus may contain nontrivial information about the potential. We do not rely on the accelerations determined directly from the data by Ghez et al. 2000, as this was done in the constant acceleration approximation which we think is not reliable. Indeed, the Newtonian predictions for the acceleration vary substantially, both in magnitude and direction, during the six years of observation. In view of this fact, we prefer to work with the raw data directly, trying to fit the projected positions in right ascension (RA) and declination of the stars in the BH and FB scenarios. For our analysis we have selected only two stars, S0-1 and S0-2, because their projected distances from SgrA* in 1995.53, 4.42 mpc and 5.83 mpc, respectively, make it most likely that these could be orbiting within a FB of radius ~ 18 mpc. We thus may in principle distinguish between the BH and FB scenarios for these two stars. The third star,

S0-4, that had in 1995.53 a projected distance of 13.15 mpc from Sgr A*, and was moving away from Sgr A* at a projected velocity of $\sim 990 \text{ km s}^{-1}$, is now definitely outside a FB with a radius ~ 18 mpc. One would thus not be able to distinguish the two scenarios for a large part of the orbit of S0-4.

In the following, we perform a detailed analysis of the orbits of the stars S0-1 and S0-2, based on the Ghez et al. 1998 and 2000 data, including the error bars of the measurements, and varying the unknown components of the position and velocity vectors of the stars in 1995.4, z and v_z . For simplicity, we assume throughout this paper that the supermassive compact dark object has a mass of $2.6 \times 10^6 M_\odot$, and is centered at the position of Sgr A* which is taken to be at a distance of 8 kpc from the sun. In fact, because of the small proper motion $\lesssim 20 \text{ km s}^{-1}$ of Sgr A*, there are strong dynamical reasons to assume in the BH scenario, that Sgr A* and the supermassive BH are at the same position, while in the FB scenario, Sgr A* and the FB could be off-center by a few mpc without affecting the results. We do not vary the mass of the supermassive compact dark object, as the calculations are not very sensitive to this parameter, as long as the mass is within the range of the error bar inferred from the statistical data on the proper motion of the stars in the central cluster (Ghez et al. 1998).

This paper is organized as follows: In section 4, we present the main equations for the description of the supermassive compact dark object as a FB, as well as the formalism for the description of the dynamics of the stars in the gravitational field of a FB or a BH. We then investigate, in section 5, the dynamics of S0-1 and S0-2, based on the Ghez et al. 2000 data, and conclude with a summary and outlook in section 6.

4. The dynamics of the stars near the Galactic center

As the stars near the Galactic center have projected velocities $\lesssim 1,400 \text{ km s}^{-1}$, one may very well describe their dynamics in terms of Newtonian mechanics for both the BH and the FB scenarios. Similarly, fermions of mass $m_f \sim 13 \text{ keV}/c^2$ to $\sim 17 \text{ keV}/c^2$, which are condensed in a degenerate FB of $(2.6 \pm 0.2) \times 10^6 M_\odot$, are nonrelativistic, since their local Fermi velocity is certainly smaller than the escape velocity of $\sim 1,700 \text{ km s}^{-1}$ from the center of the FB. The fermions will, therefore, obey the equation of hydrostatic equilibrium, the Poisson equation and the nonrelativistic equation of state of degenerate fermionic matter

$$P_f = K n_f^{5/3} \quad (1)$$

with

$$K = \frac{\hbar^2}{5m_f} \left(\frac{6\pi^2}{g_f} \right)^{2/3}. \quad (2)$$

Here, P_f and n_f , denote the local pressure and particle number density of the fermions, respectively. FBs have been discussed extensively in a number of papers (e.g. Viollier 1994; Bilić, Munyaneza and Viollier 1999; Tsiklauri and Viollier 1999). Here we merely quote the equations that we need further below, in order to make this paper self-contained. The gravitational potential of a degenerate FB is given by

$$\Phi(r) = \begin{cases} \frac{GM_\odot}{a} \left(v'(x_0) - \frac{v(x)}{x} \right) & , \quad x \leq x_0 \\ -\frac{GM}{ax} & , \quad x > x_0 \end{cases} \quad (3)$$

where a is an appropriate unit of length

$$a = \left(\frac{3\pi\hbar^3}{4\sqrt{2} m_f^4 g_f G^{3/2} M_\odot^{1/2}} \right)^{2/3} = 0.94393 \text{ pc} \left(\frac{15 \text{ keV}}{m_f c^2} \right)^{8/3} g_f^{-2/3}, \quad (4)$$

$r = ax$ is the distance from the center of the FB and $R = ax_0$ the radius of the FB. The dimensionless quantity $v(x)$, that is related to the gravitational potential $\Phi(r)$ through

eq.(3), obeys the Lané-Emden differential equation

$$\frac{d^2v}{dx^2} = - \frac{v^{3/2}}{x^{1/2}} , \quad (5)$$

with polytropic index $n = 3/2$. For a pure FB without a gravitational point source at the center, the boundary conditions at the center and the surface of the FB are $v(0) = v(x_0) = 0$. All the relevant quantities of the FB can be expressed in terms of v and x , e.g. the matter density as

$$\rho = \frac{\sqrt{2}}{3} \frac{m_f^4 g_f}{\pi^2 \hbar^3} \left(\frac{GM_\odot}{a} \right)^{3/2} \left(\frac{v}{x} \right)^{3/2} , \quad (6)$$

where m_f and g_f are the mass and the spin degeneracy factor of the fermions and antifermions, respectively, i.e. $g_f = 2$ for Majorana and $g_f = 4$ for Dirac fermions and antifermions. Based on eqs.(5) and (6), the mass enclosed within a radius r in a FB is given by

$$M(r) = \int_0^r 4\pi \rho r^2 dr = - M_\odot (v'(x)x - v(x)) , \quad (7)$$

and the total mass of the FB by

$$M = M(R) = - M_\odot v'(x_0) x_0 . \quad (8)$$

From eq.(5), one can derive a scaling relation for the mass and radius of a nonrelativistic FB, i.e.

$$\begin{aligned} MR^3 &= x_0 |v'(x_0)| x_0^3 a^3 M_\odot = \frac{91.869 \hbar^6}{G^3 m_f^8} \left(\frac{2}{g_f} \right)^2 \\ &= 27.836 M_\odot \left(\frac{15 \text{ keV}}{m_f c^2} \right)^8 \left(\frac{2}{g_f} \right)^2 (\text{pc})^3 . \end{aligned} \quad (9)$$

Here $v(x)$ is the solution of eq.(5) with $v(0) = 0$ and $v'(0) = 1$, yielding $v(x_0) = 0$ again at $x_0 = 3.65375$, and $v'(x_0) = -0.742813$. The precise index of the power law of the scaling relationship (9) depends on the polytropic index of the equation of state (1). As the mass of the FB approaches the OV limit, this scaling law is no longer valid, because the degenerate fermion gas has to be described by the correct relativistic equation of state and Einstein's

equations for the gravitational field and hydrostatic equilibrium (Bilić, Munyaneza & Viollier 1999).

We now turn to the description of the dynamics of the stars near the Galactic center. The mass of the BH and FB is taken to be $M = 2.6 \times 10^6 M_\odot$. In order to emphasize the differences between the FB and the BH scenarios, we choose the fermion masses $m_f = 15.92 \text{ keV}/c^2$ for $g_f = 2$ or $m_f = 13.39 \text{ keV}/c^2$ for $g_f = 4$. These are the minimal fermion masses consistent with the mass distribution inferred from the statistics of proper motions of the stars in the central cluster (Munyaneza, Tsiklauri and Viollier, 1999; Ghez et al. 1998). The dynamics of the stars in the gravitational field of the supermassive compact dark object can be calculated solving Newton's equations of motion

$$\ddot{\vec{r}} = -\frac{GM(r)}{r^3} \vec{r}, \quad (10)$$

taking into account the position and velocity vectors at e.g. $t_0 = 1995.4$ yr, i.e. $\vec{r}(t_0) \equiv (x, y, z)$ and $\dot{\vec{r}}(t_0) \equiv (v_x, v_y, v_z)$. For the FB scenario, $M(r)$ is given by eq.(7), while in the BH case it is replaced by M of eq.(8). The x -axis is chosen in the direction opposite to the right ascension (RA), the y -axis in the direction of the declination, and the z -axis points towards the sun. The BH and the center of the FB are assumed to be at the position of Sgr A* which is also the origin of the coordinate system at an assumed distance of 8 kpc from the sun.

5. Analysis of the orbits of S0-1 and S0-2

In 1995.4, the projected positions and velocities of S0-1 reported by Ghez et al. 1998, were $x = -0.107''$, $y = 0.039''$, $v_x = (470 \pm 130) \text{ km s}^{-1}$ and $v_y = (-1330 \pm 140) \text{ km s}^{-1}$. We now investigate how the projected orbits, calculated using eq.(10), are affected by (i) the error bars of v_x and v_y of S0-1 measured in 1995.4, (ii) the lack of knowledge of z of

S0-1 in 1995.4, (iii) the lack of information on v_z of S0-1 in 1995.4. We then compare the results with the S0-1 data recently reported by Ghez et al. 2000.

Fig.1 shows the RA of S0-1 as a function of time, taking into account the error bars of v_x and v_y and choosing $z = v_z = 0$ in 1995.4. The top panel represents the RA of S0-1 in the BH scenario, while the bottom panel illustrates the same quantities in the FB case. From Fig.1 we conclude that, for $z = v_z = 0$ in 1995.4, the error bars of v_x and v_y of 1995.4 do not allow for a fit of the new Ghez et al. 2000 data of S0-1 in the BH scenario, whereas the data are described quite easily within the error bars in the FB case. In Fig.2, the declination is plotted as a function of time for the same values of v_x , v_y , z and v_z in 1995.4. We arrive at the same conclusion as in Fig.1: For $z = v_z = 0$ the error bars of v_x and v_y allow for a fit of the data in the FB scenario only.

As a next step, the sensitivity of the orbits to the z - coordinate of S0-1 in 1995.4 is investigated. To this end, we restrict ourselves to bound orbits of S0-1 only. The conserved total energy of the star S0-1 is given by

$$E = \frac{1}{2}m \dot{r}^2 + m\Phi(r) , \quad (11)$$

where the unknown star mass can be chosen as $m = 1$ without loss of generality. S0-1 is unlikely to have a total energy $E > 0$, because, in the absence of swing-by events caused by stars of the central cluster, S0-1 will have to fall in with a velocity that is inconsistent with the velocity dispersion of the stars at infinity. The condition $E \leq 0$ thus yields upper limits, $|v_z| \leq |v_z^\infty|$ and $|z| \leq |z_\infty|$, which depend on v_x and v_y as can be seen from Table 1. In this context, it is worthwhile to note that, at a radius equal to the projected distance of S0-1 to Sgr A* in 1995.4, the escape velocity from a BH is $2,250 \text{ km s}^{-1}$, while that from a FB is $1,613 \text{ km s}^{-1}$. The escape velocity from the center of the FB is $1,672 \text{ km s}^{-1}$.

Fig. 3 presents the sensitivity of the RA of S0-1 with respect to the z -coordinate in both the BH and FB scenarios. In the case of a BH, the RA depends strongly on the value

of z in 1995.4, while the z -dependence in the FB scenario is rather weak. In both the top and bottom panels, $v_x = 340 \text{ km s}^{-1}$, $v_y = -1190 \text{ km s}^{-1}$ and $v_z = 0$ has been assumed while z is varied, all in 1995.4 values. In the BH scenario, none of the other input values for v_x and v_y would fit the new Ghez et al. 2000 data if we restrict ourselves to bound orbits. In the FB case, the input values $v_x = 340 \text{ km s}^{-1}$ and $v_y = -1470 \text{ km s}^{-1}$ describe the Ghez et al. 2000 data as well as $v_x = 340 \text{ km s}^{-1}$ and $v_y = -1190 \text{ km s}^{-1}$. Looking at Fig. 3, we thus conclude that the RA data of S0-1 are well fitted with $|z| \approx 0.25''$ in the BH scenario, and with $|z| \lesssim 0.1''$ in the FB case. The dependence of the declination on z is shown in Fig.4. In order to describe the Ghez et al. 2000 data for the declination of S0-1, we require $0.25'' \lesssim |z| \lesssim |z_\infty| = 0.359''$ for the BH scenario, while in the FB case, the declination can be fitted with $|z| \lesssim 0.359''$.

Fig.5 represents an investigation of how the RA of S0-1 is affected by v_z of 1995.4. In this graph we have chosen $v_x = 340 \text{ km s}^{-1}$, $v_y = -1190 \text{ km s}^{-1}$ and $z = 0$ in 1995.4. Increasing $|v_z|$ up to its maximal value $|v_z^\infty| = 1879 \text{ km s}^{-1}$ does not help fitting the RA data of S0-1 in the BH scenario. In the FB case, the orbits are rather insensitive to $|v_z|$. Thus all $|v_z| \lesssim |v_z^\infty| = 1036 \text{ km s}^{-1}$ fit the RA data of S0-1 quite well. The weak dependence of the RA on $|v_z|$ in the FB scenario is due to the harmonic oscillator like shape of the FB potential at small distances, where the Newtonian equations of motion nearly decouple in Cartesian coordinates. Fig.6 exhibits the declination as a function of time for various values of $|v_z|$, keeping v_x , v_y and z in 1995.4 as in Fig.5. The top panel of Fig.6 shows that increasing $|v_z|$ from zero up to its maximal value $|v_z^\infty| = 1879 \text{ km s}^{-1}$ barely helps fitting the data in the BH scenario. In the FB scenario, the declination may be described by $|v_z| \lesssim 900 \text{ km s}^{-1}$.

Summarizing the results of Figs.3-6, we can plot in Fig.7 the $z - v_z$ phase-space of 1995.4 that fits the data. The small range of acceptable $|z|$ and $|v_z|$ values in the BH

scenario (solid vertical line) reflects the fact that the orbits of S0-1 depend strongly on these two parameters. Conversely, the weak dependence of the orbits on $|z|$ and $|v_z|$ in the FB case is the reason for the much larger $z - v_z$ phase-space that is fitting the Ghez et al. 2000 data of S0-1, as shown by the dashed box. The dashed and solid curves describe the $E = 0$ (just bound) orbit in the FB and BH scenarios, respectively.

Fig.8 shows some typical projected orbits of S0-1 in the BH and FB scenarios. The Ghez et al. 2000 data of S0-1 may be fitted in both scenarios with appropriate choices of v_x , v_y , z and v_z in 1995.4. The inclination angles of the orbit's plane $\theta = \arccos(L_z/|\vec{L}|)$, with $\vec{L} = m\vec{r} \times \dot{\vec{r}}$, are shown next to the orbits. The minimal inclination angle that describes the data in the BH case is $\theta = 70^\circ$, while in the FB scenario it is $\theta = 0^\circ$. In the BH case, the minimal and maximal distances from Sgr A* are $r_{min} = 0.25''$ and $r_{max} = 0.77''$, respectively, for the orbit with $z = 0.25''$ and $v_z = 0$ which has a period of $T \approx 161$ yr. The orbits with $z = 0.25''$ and $v_z = 400 \text{ km s}^{-1}$ or $z = 0.25''$ and $v_z = 700 \text{ km s}^{-1}$ have periods of $T \approx 268$ yr or $T \approx 3291$ yr, respectively. In the FB scenario, the open orbit with $z = 0.1''$ and $v_z = 0$ has a “period” of $T \approx 77$ yr with $r_{min} = 0.13''$ and $r_{max} = 0.56''$. The open orbits with $z = 0.1''$ and $v_z = 400 \text{ km s}^{-1}$ or $z = 0.1''$ and $v_z = 900 \text{ km s}^{-1}$ have “periods” of $T \approx 100$ yr or $T \approx 1436$ yr, respectively.

Fig.9 is a prediction of $|v_z|$ as a function of time for both the BH and FB scenarios and various acceptable input parameters (see Fig.7). This shows that the radial velocity $|v_z|$ of S0-1, if measured in a few years time, could serve to distinguish between the BH and the FB scenarios. For the BH case, we predict by the year 2005 a radial velocity $|v_z| \lesssim 900 \text{ km s}^{-1}$, while in the FB scenario the radial velocity will be $|v_z| \lesssim 500 \text{ km s}^{-1}$. Radial velocities $|v_z| \gtrsim 1000 \text{ km s}^{-1}$ before 2010 would be excluded in both the BH and FB scenarios.

We now repeat the analysis in the case of the star S0-2. The x - and y -components of the position and velocity vectors of S0-2 at $t_0 = 1995.4$ yr are $\vec{r}(t_0) = (0.007'', 0.151'')$

and $\dot{\vec{r}}(t_0) = (-290 \pm 110, -500 \pm 50) \text{ km s}^{-1}$, respectively (Ghez et al. 1998). Restricting ourselves to bound orbits, the Ghez et al. 2000 data of S0-2 can be fitted in the BH scenario, with $v_x = -290 \text{ km s}^{-1}$, $v_y = -500 \text{ km s}^{-1}$, $|z| \approx 0.25''$ and $|v_z| \lesssim 1280 \text{ km s}^{-1}$ in 1995.4. In the FB scenario, the allowed $z - v_z$ phase-space is $|z| \lesssim 0.1''$ and $|v_z| \lesssim 1000 \text{ km s}^{-1}$ for the same values of v_x and v_y in 1995.4. The range of acceptable values of $|z|$ and $|v_z|$ is shown in Fig.10, where the solid and dashed curves denote the limits on $|z|$ and $|v_z|$ for $E = 0$ (just bound) orbits in the BH and FB cases, respectively. Here again the $z - v_z$ phase-space turns out to be much larger in the FB (dashed box) than in the BH scenario (vertical solid line).

Fig.11 exhibits some typical projected orbits of S0-2 corresponding to the acceptable $z - v_z$ phase-space of Fig.10 in both the BH and FB scenarios. Next to the orbits the inclination angles of the orbit's plane are shown. In the BH scenario, the lower limit of the inclination angle is $\theta = 74^\circ$, for the orbit (1) with $z = 0.25''$ and $v_z = 0$. The minimal and maximal distances from the center are $r_{min} = 0.045''$ and $r_{max} = 0.307''$, respectively. The period of this closed orbit is minimal with $T \approx 34 \text{ yr}$. However, this value disagrees with the minimal period $T \approx 16 \text{ yr}$ quoted by Ghez et al. 2000. The orbit (2) with $z = 0.25''$ and $v_z = 500 \text{ km s}^{-1}$ or $z = 0.25''$ and $v_z = 1000 \text{ km s}^{-1}$ have periods $T \approx 42 \text{ yr}$ or $T \approx 135 \text{ yr}$, respectively. In the FB scenario the minimal inclination angle of the orbit's plane is $\theta = 0^\circ$. The open orbit (1) with $z = 0.25''$ and $v_z = 0$ has minimal and maximal distances from the center of $r_{min} = 0.15''$ and $r_{max} = 0.31''$, respectively, with a “period” of $T \approx 46 \text{ yr}$. The open orbits with (1) $z = 0.25''$ and $v_z = 500 \text{ km s}^{-1}$ or (2) $z = 0.25''$ and $v_z = 1000 \text{ km s}^{-1}$ have “periods” $T \approx 51 \text{ yr}$ or $T \approx 174 \text{ yr}$, respectively. The minimal “period” $T \approx 37 \text{ yr}$ is obtained for an open orbit with $z = v_z = 0$ and inclination angle $\theta = 0^\circ$.

In Fig. 12 the predictions for the radial velocity $|v_z|$ are plotted as a function of time for various acceptable input values of z and v_z in 1995.4. It is seen that a radial velocity of

$|v_z| \gtrsim 1000 \text{ km s}^{-1}$ is excluded in the FB scenario.

6. Summary and outlook

In this paper, we have shown that the orbits of S0-1 and S0-2, observed by Ghez et al. 2000 during the last six years, are consistent with either a BH or a FB of $2.6 \times 10^6 M_\odot$ at the center of the Galaxy. In order to fit the data in the BH scenario, S0-1 and S0-2 must have had in 1995.4 a z -coordinate of $|z| \approx 0.25''$ and radial velocities of $|v_z| \lesssim 750 \text{ km s}^{-1}$ or $|v_z| \lesssim 1280 \text{ km s}^{-1}$ for S0-1 or S0-2, respectively. In the BH scenario, the orbits of S0-1 and S0-2 strongly depend on z in 1995.4. The new data of S0-1 and S0-2 can be fitted in the FB scenario with $z = v_z = 0$ in 1995.4. Due to the weak dependence of the orbits on $|z|$ and $|v_z|$ in the FB case, $|z| \lesssim 0.1''$ and $|v_z| \lesssim 900 \text{ km s}^{-1}$ for S0-1 or $|z| \lesssim 0.25''$ and $|v_z| \lesssim 1000 \text{ km s}^{-1}$ for S0-2 are also consistent with the Ghez et al. 2000 data. As new measurements become available, the acceptable $z - v_z$ phase-space of 1995.4 could be further constrained.

We have plotted some typical orbits of S0-1 and S0-2 in both the BH and FB scenarios and have shown that the minimal inclination angle of the orbit's plane is $\theta = 70^\circ$ as in the BH case and $\theta = 0^\circ$ in the FB scenario. We have established that by the year 2005, the measurement of the radial velocities $|v_z|$ of both S0-1 and S0-2 could discriminate between the two scenarios of the supermassive compact dark object at the Galactic center. In concluding, it is important to note again that, based on the Ghez et al. 2000 data of the stars S0-1 and S0-2, the FB scenario cannot be ruled out. On the contrary, in view of the $z - v_z$ phase-space, that is much larger in FB scenario than in the BH case, there is reason to treat the FB scenario of the supermassive compact dark object at the center of our Galaxy with the respect it deserves.

We now turn to the discussion of promising techniques for proving or disproving the

FB or BH scenarios of the Galactic center. These can be basically divided into two classes:

- (i) probing the gravitational potential at distances $\lesssim 0.5''$ from the Galactic center, and
- (ii) observing the decay or the annihilation of the fermions of the FB into visible particles, at distances $\lesssim 0.5''$ from the Galactic center.

In the first category, the most promising method is still monitoring the proper motions and radial velocities of stars that are located at projected distances $\lesssim 0.5''$ from Sgr A*, as well as interpreting these observations in terms of the FB or BH scenarios. However, a further interesting possibility is the observation of gravitationally lensed stars in the line of sight behind the FB (Bilić, Nikolić and Viollier 2000), as a FB of ~ 18 mpc radius is a much more efficient gravitational lens than a BH of the same mass. In fact, a star crossing the line of sight with a minimal distance of ~ 0.2 mpc, ~ 200 pc behind the center of the FB, will produce for a few years up to three distinct moving images within or just outside the Einstein ring radius of $\sim 0.13''$ or ~ 5 mpc. Two of these star images will pop out of nothing at some point inside the Einstein ring, and they will first separate, then approach each other again and finally annihilate each other at a different point within the Einstein ring. The third image moves around the Einstein ring while the projection of the source crosses the ring area. Unfortunately, the rate for such a remarkable event, which would be the smoking gun for an extended supermassive object, is estimated to be only $\sim 10^{-4}/\text{yr}$. In the BH case, the manifestations of gravitational lensing are less spectacular with only two observable lensed moving images (Wardle and Yusef-Zadeh 1992). Another possible test of the gravitational potential could be the spectrum of the radiation emitted by the accreted baryonic matter, once the model dependence of the calculations can be controlled.

In the second category, the particle content of FBs could be proven e.g. through the radiative decay of the fermion (assumed here to be a sterile neutrino) into a standard

neutrino, i.e. $f \rightarrow \nu\gamma$. If the lifetime for this decay is 1.4×10^{18} yr, the luminosity of the FB would be 4×10^{34} erg/sec. The signal would be a sharp X-ray line of ~ 8 keV for $g_f = 2$ or ~ 7 keV for $g_f = 4$. The X-ray luminosity would be tracing the fermion matter density. Of course the spatial resolution of the X-ray telescope would have to be $\lesssim 0.5''$. A further possible test could be the annihilation of two fermions into two or three photons, i.e. $f\bar{f} \rightarrow \gamma\gamma$ or $f\bar{f} \rightarrow \gamma\gamma\gamma$. However, the branching ratios of these two annihilation processes with respect to a presumably dominant but unobservable $f\bar{f} \rightarrow \nu'\bar{\nu}'$ channel are most probably too small to be observable. Nevertheless, the signal would be a sharp line of ~ 16 keV ($g_f = 2$) or ~ 14 keV ($g_f = 4$) for $f\bar{f} \rightarrow \gamma\gamma$, and a continuous spectrum with a maximum at ~ 10 keV ($g_f = 2$) or ~ 9 keV ($g_f = 4$) for $f\bar{f} \rightarrow \gamma\gamma\gamma$. For s-wave annihilation the X-ray luminosity would trace the square of the fermion matter density, while for p-wave annihilation the concentration of the X-ray emission towards the center of the FB would be even more pronounced.

Acknowledgements

This work is supported in part by the Foundation for Fundamental Research (FFR) grant number PHY 99-01241. F. Munyaneza gratefully acknowledges the financial support from the British Department of Social Security (DSS). We have enjoyed valuable discussions with N. Bilić, T. Koch, D. Tsiklauri and G.B. Tupper.

REFERENCES

Alcock, C. 2000, *Science*, 287, 74

Backer, D.C. 1996, in *Unsolved problems in the Milky Way*, eds.L. Blitz and P. Teuben, Proc. of IAU Symp. No. 169 (Dordrecht: Kluwer)

Backer, D. C., Sramek, R. A., 1999, *ApJ*, 524, 805

Baganoff, F., et al. 1999, *American Astronomical Society Meeting*, 195, 6201

Bilić, N., Lindebaum, R. J., Tupper, G. B., Viollier, R. D. 2000, *astro-ph/0008230*

Bilić, N., Munyaneza, F., Viollier, R.D. 1999, *Phys. Rev. D*, 59, 024003

Bilić, N., Nikolić, H., Viollier, R. D. 2000, *ApJ*, 537, 909

Bilić, N., Tsiklauri, D.G., Viollier, R.D. 1998, *Prog. Part. Nucl. Phys.*, 40, 17

Bilić, N., Viollier, R.D. 1997, *Phys. Lett. B*, 408,75

Bilić, N., Viollier, R.D. 1998, *Nucl. Phys. (Proc. Suppl.) B*, 66,256

Bilić, N., Viollier, R.D. 1999a, *Gen. Relativ. Grav.*, 31, 1105

Bilić, N., Viollier, R.D. 1999b, *Eur. Phys. J. C*, 11, 173

Bower, G.C. Backer, D.C. 1998, *ApJ*, 496, L97

Chun, E. J., Kim, H. B. 1999, *Phys. Rev. D*, 60, 095006

Dressler, A. Richstone, D.O., 1988, *ApJ*, 324, 701

Eckart, A., Genzel, R. 1996, *Nature*, 383,415

Eckart, A., Genzel, R. 1997, *MNRAS*, 284, 576

Falcke, H., Biermann, P. L. 1996, A&A, 308, 321

Falcke, H., Biermann, P. L. 1999, A&A, 342, 49

Falcke, H., Mannheim, K., Biermann, P. L. 1993, A&A, 278, L1

Ford, H.C., et al. 1994, ApJ, 435, L27

Fukuda, S., et al. 2000, Phys. Rev. Lett., 85, 3999

Genzel, R., Eckart, A., Ott, T., Eisenhauer, F. 1997, MNRAS, 291, 219

Genzel, R., Eckart, A. 1999, in Proc. The Central Parsecs of the Galaxy, eds. Falcke, H., Cotera, A., Duschl, W., Melia, F., Rieke, M., ASP Conf.Series, Vol. 186

Genzel, R., Hollenbach, D.J., Townes, C.H. 1994, Rep. Prog. Phys., 57, 417

Genzel, R., Pichon, C., Eckart, A., Gerhard, O. E. & Ott, T. 2000, MNRAS, 317, 418

Genzel, R., Thatte, N., Krabbe, A., Kroker, H., & Tacconi-Garman, L.E. 1996, ApJ, 472, 153

Genzel, R., & Townes, C.H. 1987, ARA&A, 25, 377

Ghez, A.M., Klein, B.L., Morris, M., & Becklin, E.E. 1998, ApJ, 509, 678

Ghez, A. M., Morris, M., Becklin, E. E., Tanner, A., & Kremenek, T. 2000, Nature, 407, 351

Giudice, G.F. et al. 2000, hep-ph/0012317.

Goldwurm, A. et al. 1994, Nature, 371, 589

Gondolo, P. & Silk, J. 1999, Phys. Rev. Lett. 83, 1719

Goto, T., & Yamaguchi, M. 1992, Phys. Lett., B276, 123

Greenhill, L.J., Jiang, D.R., Moran, J.M., Reid, M.J., Lo, K.Y., & Claussen, M.J. 1995, ApJ, 440, 619

Haller, J. W., Rieke, M. J., Rieke, G.H., Tamblyn, P., Close, L., & Melia, F. 1996, ApJ, 456, 194

Harms, R. J., et al. 1994, ApJ, 435, L35

Ho, L. C., & Kormendy, J., 2000, in Encyclopedia of Astronomy and Astrophysics, ed. Institute of Physics Publishing, astro-ph/0003267

Kormendy, J. 1988, ApJ, 325, 128

Kormendy, J. 2000, Nature, 407, 307

Kormendy, J., & Richstone, D. 1995, ARA&A, 33, 581

Kormendy, J., & Ho, L.C., 2000, in Encyclopedia of Astronomy and Astrophysics, ed. Institute of Physics Publishing, astro-ph/0003268

Koyama, K., et al., 1996, PASJ, 48, 249

Krichbaum, T.P. et al. 1994, in Compact Extragalactic Radio Sources (Proc. NRAO Workshop, Socorro, New Mexico), ed. J.A. Zensur and K.I. Kellermann (Greenbank: NRAO), 39

Lo, K. Y., Shen, Z.-Q., Zhao, J.H., & Ho, P. T. 1998, ApJ, 508, L61

Lyth, D.H., hep-ph/9911257

Macchetto, F., et al. 1997, ApJ, 489, 579

Mahadevan, R. 1998, Nature, 394, 651

Maoz, E. 1995, ApJ, 447, L91

Maoz, E. 1998, ApJ, 494, L181

Melia, F. 1994, ApJ, 426, 577

Morris, M., & Serabyn, E. 1996, ARA&A, 34, 645

Munyaneza, F., Tsiklauri, D., & Viollier, R. D. 1998, ApJ, 509, L105

Munyaneza, F., Tsiklauri, D., & Viollier, R. D. 1999, ApJ, 526, 744

Munyaneza, F. & Viollier, R.D., astro-ph/9907318

Myoshi, M., Moran, J. M., Hernstein, J., Greenhill, L., Nakai, N.,Diamond, P., Inoue, M. 1995, Nature, 373, 127

Narayan, R., et al. 1998, ApJ, 492, 551

Narayan, R., Yi, I., & Mahadevan, R. 1995, Nature, 374, 623

Navarro, J.F., Frenk, C.S. & White, S.D.M. 1997, ApJ, 490, 493

Predehl, P., & Trümper, J. 1994, ApJ, 509, 678

Reid, M. J., Readhead, A. C. S., Vermeulen, R. C., Treuhaft, R. N. 1999, ApJ, 524, 816

Richstone, D., et al. 1998, Nature, 394, A14

Rogers, A.E.E., et al. 1994, ApJ, 434, L59

Roszkowski, L. 2001, hep-ph/0102327

Sanders, R. H. 1992, Nature, 359, 131

Shi, X., & Fuller, G. M. 1999, Phys. Rev. Lett., 82, 2823

Sidoli, L., & Mereghetti, S. 1999, A&A, 349, L49

Sunyaev, V., et al. 1993, ApJ, 407, 603

Tsiklauri, D., & Viollier, R.D. 1996, MNRAS, 282, 1299

Tsiklauri, D., & Viollier, R.D. 1998a, ApJ, 500, 591

Tsiklauri, D., & Viollier, R.D. 1998b, ApJ, 501, 486

Tsiklauri, D., & Viollier, R.D. 1999, Astropart. Phys., 12, 199

Tupper, G.B., Lindebaum, R.J. & Viollier, R.D. 2000, Mod. Phys. Lett. A, 15, 1221

Viollier, R.D. 1994, Prog. Part. Nucl. Phys., 32, 51

Viollier, R.D., Leimgruber, F.R., & Trautmann, D. 1992, Phys. Lett. B, 297, 132

Viollier, R.D., Trautmann, D., & Tupper, G.B., 1993, Phys. Lett. B, 306, 79

Wardle, M., & Yusef-Zadeh, F., 1992, ApJ, 387, L65

Yusef-Zadeh, F., Melia, F. & Wardle, M. 2000, Science, 287, 85

Figure captions:

Fig.1 : The RA of S0-1 as a function of time, taking into account the error bars of the projected velocity in 1995.4 (Ghez et al. 98). The top panel is drawn for the case of a black hole (BH), while the bottom panel corresponds to a fermion ball (FB), both centered at Sgr A*. The labels of the graphs stand for the velocity components: (1) $v_x = 470 \text{ km s}^{-1}$, $v_y = -1330 \text{ km s}^{-1}$ (median values); (2) $v_x = 340 \text{ km s}^{-1}$, $v_y = -1190 \text{ km s}^{-1}$; (3) $v_x = 340 \text{ km s}^{-1}$, $v_y = -1470 \text{ km s}^{-1}$; (4) $v_x = 600 \text{ km s}^{-1}$, $v_y = -1190 \text{ km s}^{-1}$; (5) $v_x = 600 \text{ km s}^{-1}$, $v_y = -1470 \text{ km s}^{-1}$, all for 1995.4. In this plot, z and v_z are taken to be zero in 1995.4. One thus concludes that, within the error bars of the projected velocities of 1995.4, the data points recently reported by Ghez et al. 2000 can be fitted in the FB scenario with $v_z = z = 0$ (lines 2 and 3), while this is not the case in the BH scenario. In this figure, the masses of both the FB and the BH, are $M = 2.6 \times 10^6 M_\odot$. The fermion mass is taken to be $m_f c^2 = 15.92 \text{ keV}$ with a degeneracy factor of $g_f = 2$, or $m_f c^2 = 13.39 \text{ keV}$ with $g_f = 4$. Fig.2: This is an analysis similar to that of Fig.1 but for the declination of S0-1 as a function of time. Assuming $v_z = z = 0$ in 1995.4, the data points can be represented within the error bars of v_x and v_y in 1995.4 in the FB scenario only. Fig. 3: Here we investigate the dependence of the RA of S0-1 on the z -coordinate. The data can be described with $v_x = 340 \text{ km s}^{-1}$, $v_y = -1190 \text{ km s}^{-1}$, $v_z = 0$ and $|z| \approx 0.25''$ in the BH case. In the FB scenario, the data can be fitted for the same values of v_x , v_y , v_z and $|z| \lesssim 0.1''$. We note that the RA strongly depends on z in the BH case, while in the FB scenario the dependence on z is rather weak, as the equations of motion nearly decouple for small x , y , and z . The limit value $|z_\infty| = 0.359''$ corresponds to a just bound orbit with total energy $E = 0$ and $v_z = 0$ (see Table 1). Fig.4 : The dependence of the declination of S0-1 on $|z|$ for $v_z = 0$, $v_x = 340 \text{ km s}^{-1}$ and $v_y = -1190 \text{ km s}^{-1}$, all in 1995.4 values. The declination can be fitted from $|z| \approx 0.25''$ to $|z_\infty| = 0.359''$ in the BH case. In the FB scenario all values $|z| \lesssim 0.359''$ fit the data. Fig.5: Here we explore how the RA of S0-1 depends on $|v_z|$ while keeping $z = 0$, $v_x =$

340 km s⁻¹ and $v_y = -1190$ km s⁻¹, taken in 1995.4. Increasing $|v_z|$ up to its maximal value $|v_z^\infty| = 1879$ km s⁻¹, which corresponds to a $E = 0$ (just bound) orbit with $z = 0$, does not help fitting the data in the BH scenario. In the FB case, there is a weak dependence on v_z , and all the values $|v_z| \lesssim 1879$ km s⁻¹ describe the data. Fig.6: The declination of S0-1 as a function of $|v_z|$ for $z = 0$, $v_x = 340$ km s⁻¹ and $v_y = -1190$ km s⁻¹, all in 1995.4 values. In the BH case, the data can only be described for very large $|v_z|$, while in the FB scenario the data are fitted for $|v_z| \lesssim 900$ km s⁻¹. Fig.7: The $z - v_z$ phase-space of 1995.4 that fits the S0-1 data with $v_x = 340$ km s⁻¹ and $v_y = -1190$ km s⁻¹ in 1995.4. In the BH case, the data require $|z| \approx 0.25''$ (vertical solid line), as the orbits strongly depend on z , and $|v_z| \lesssim 750$ km s⁻¹. The large range of acceptable $|z|$ and $|v_z|$ values in the FB case, denoted by the dashed rectangular box, is due to the fact that the orbits depend weakly on these two parameters. Values of $|z| \lesssim 0.1''$ and $|v_z| \lesssim 900$ km s⁻¹ are consistent with the measured positions of S0-1 in the FB scenario. The solid and dashed curves correspond to the limits of possible values of $|z|$ and $|v_z|$ for $E = 0$ (just bound) orbits of S0-1 in the BH and FB cases, respectively. Fig.8: Examples of typical orbits of S0-1 for $v_x = 340$ km s⁻¹ and $v_y = -1190$ km s⁻¹ in 1995.4. The inclination angles of the plane of the orbit are indicated next to the curves. In the BH case, the orbit with $z = 0.25''$ and $v_z = 0$ in 1995.4 has minimal and maximal distances from Sgr A* of $r_{min} = 0.25''$ and $r_{max} = 0.77''$, respectively, with a period of $T \approx 161$ yr. The orbits with $z = 0.25''$ and $v_z = 400$ km s⁻¹ or $z = 0.25''$ and $v_z = 700$ km s⁻¹ in 1995.4 have periods of $T \approx 268$ yr or $T \approx 3291$ yr, respectively. In the FB scenario, the open orbit with $z = 0.1''$ and $v_z = 0$ has a "period" of $T \approx 77$ yr with $r_{min} = 0.13''$ and $r_{max} = 0.56''$. The open orbit with $z = 0.1''$ and $v_z = 400$ km s⁻¹ in 1995.4 has a "period" $T \approx 100$ yr, while that with $z = 0.1''$ and $v_z = 900$ km s⁻¹ has a "period" of $T \approx 1436$ yr. We note that the minimal inclination angle of the orbit's plane is $\theta = 70^\circ$ in the BH case and $\theta = 0^\circ$ in the FB scenario. Fig.9: The prediction for $|v_z|$ as a function of time for S0-1. In the BH scenario with $|z| = 0.25''$ and $v_z = 0$ in 1995.4, $|v_z|$ should be

$\lesssim 900$ km s $^{-1}$ by the year 2005. The FB scenario predicts a $|v_z| \lesssim 500$ km s $^{-1}$ by the year 2005, for $v_z = 0$ and $|z| = 0.1''$ in 1995.4. Thus, once the radial velocities are measured, this figure could serve to distinguish between the BH and FB scenarios of Sgr A*. Fig. 10: The $z - v_z$ phase-space of 1995.4 that fits the S0-2 data with $v_x = -290$ km s $^{-1}$ and $v_y = -500$ km s $^{-1}$ in 1995.4. The solid and dashed curves denote the limits on $|z|$ and $|v_z|$ for $E = 0$ (just bound) orbits in the BH and FB scenarios, respectively. In the BH case, the vertical solid line at $|z| \approx 0.25''$ up the BH curve stands for the region of the allowed values of $|z|$ and $|v_z|$ for S0-2. In the FB scenario, the large allowed $z - v_z$ phase-space denoted by the dashed rectangular box, is due to the fact that the open orbits depend rather weakly on these two parameters. Fig.11: Examples of typical orbits of S0-2 for $v_x = -290$ km s $^{-1}$ and $v_y = -500$ km s $^{-1}$ in 1995.4. The labels of the orbits in both the upper (BH) and lower (FB) panels stand for: (1) $z = 0.25'', v_z = 0$; (2) $z = 0.25'', v_z = 500$ km s $^{-1}$; (3) $z = 0.25'', v_z = 1000$ km s $^{-1}$. The parameters of the label (0) $z = 0, v_z = 150$ km s $^{-1}$ fit the S0-2 data in the FB scenario only. The inclination angles of the plane of the orbit are indicated next to the curves. In the FB case, these values correspond to the maximal possible $|z|$ and $|v_z|$ in 1995.4 for bound orbits. Bearing in mind that $|z| \lesssim 0.25''$ in the FB case, the inclination angle can take any value from $\theta = 0^\circ$ to $\theta = 82^\circ$. As an example, an orbit with $\theta = 29^\circ$ with the label (0) is shown in the lower panel. However, in the BH scenario, the lower limit for the inclination angle is $\theta = 74^\circ$. The closed orbit with label (1) has $r_{min} = 0.045''$, $r_{max} = 0.307''$ and a period of $T \approx 34$ yr. The closed orbits with labels (2) and (3) have periods of $T \approx 42$ yr and $T \approx 135$ yr, respectively. The open orbit with label (1) has a “period” of $T \approx 46$ yr with $r_{min} = 0.15''$ and $r_{max} = 0.31''$. The open orbits with labels (2) and (3) have “periods” of $T \approx 51$ yr and $T \approx 174$ yr, respectively. Fig.12: The prediction for $|v_z|$ as a function of time for S0-2. This could serve to distinguish between the FB and the BH scenarios of the supermassive dark object at the Galactic center. A radial velocity $v_z \gtrsim 1000$ km s $^{-1}$ would rule out the FB scenario.

| | | black hole | | fermion ball | |
|-----------------------|-----------------------|-----------------------|--------------------------------|-----------------------|--------------------------------|
| v_x (km s $^{-1}$) | v_y (km s $^{-1}$) | $ z_\infty $ (arcsec) | $ v_z^\infty $ (km s $^{-1}$) | $ z_\infty $ (arcsec) | $ v_z^\infty $ (km s $^{-1}$) |
| 470 | -1330 | 0.27 | 1753 | 0.24 | 784 |
| 340 | -1190 | 0.359 | 1879 | 0.359 | 1036 |
| 340 | -1470 | 0.226 | 1669 | 0.165 | 572 |
| 600 | -1190 | 0.304 | 1813 | 0.295 | 910 |
| 600 | -1470 | 0.1985 | 1594 | 0.079 | 287 |

Table 1: Maximal values of $|z|$ and $|v_z|$ in 1995.4 for $E = 0$ (just unbound) orbits of S0-1.

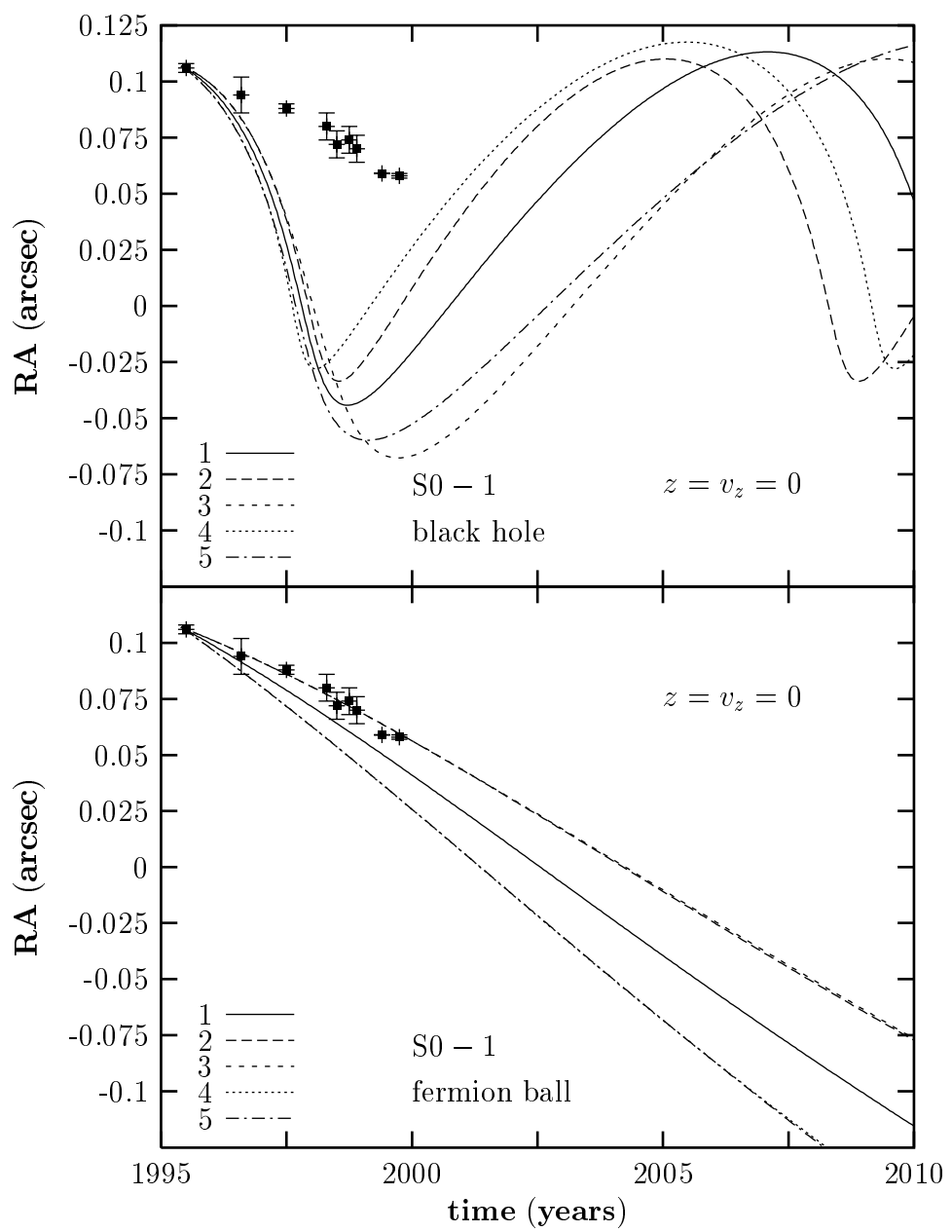


Fig.1

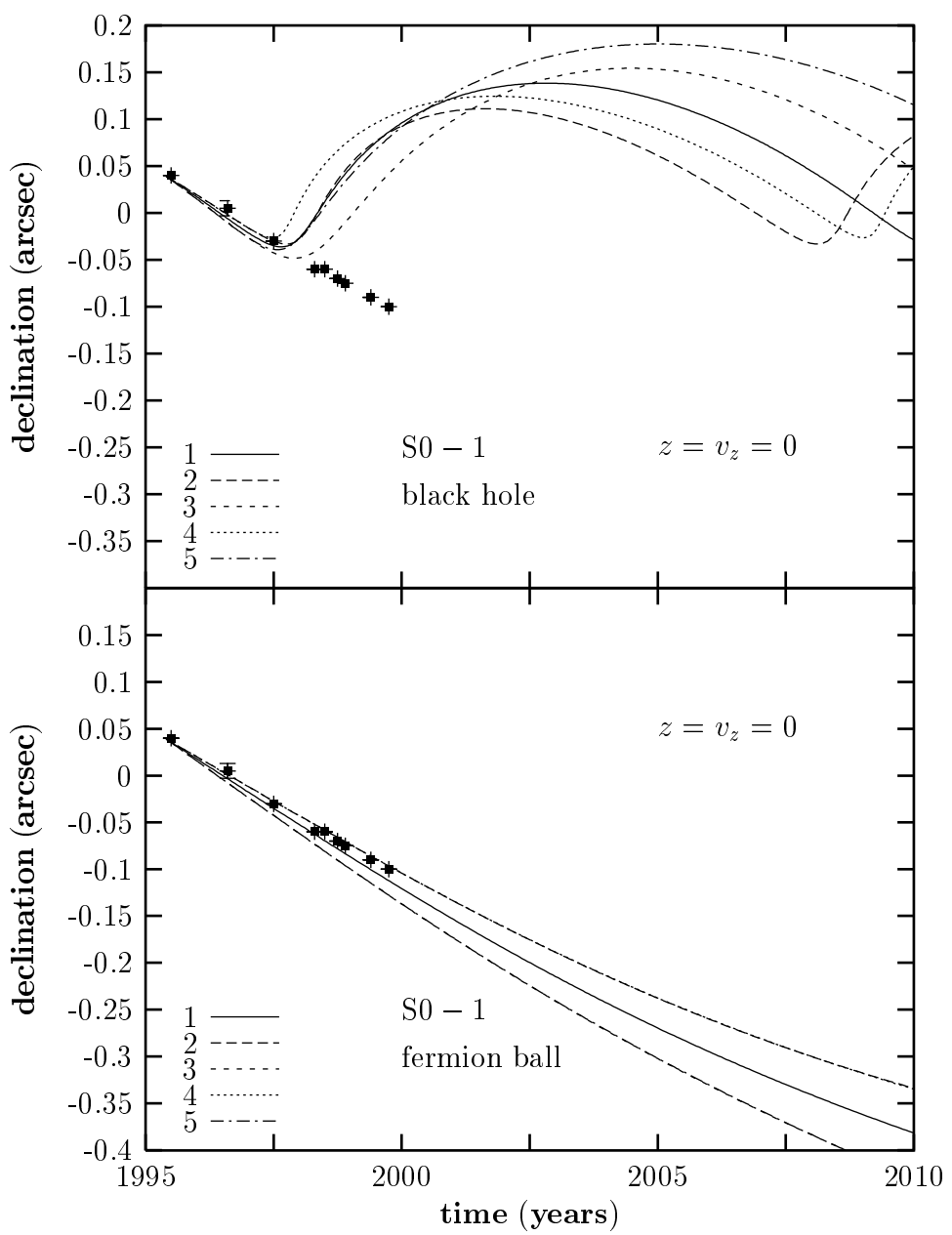


Fig.2

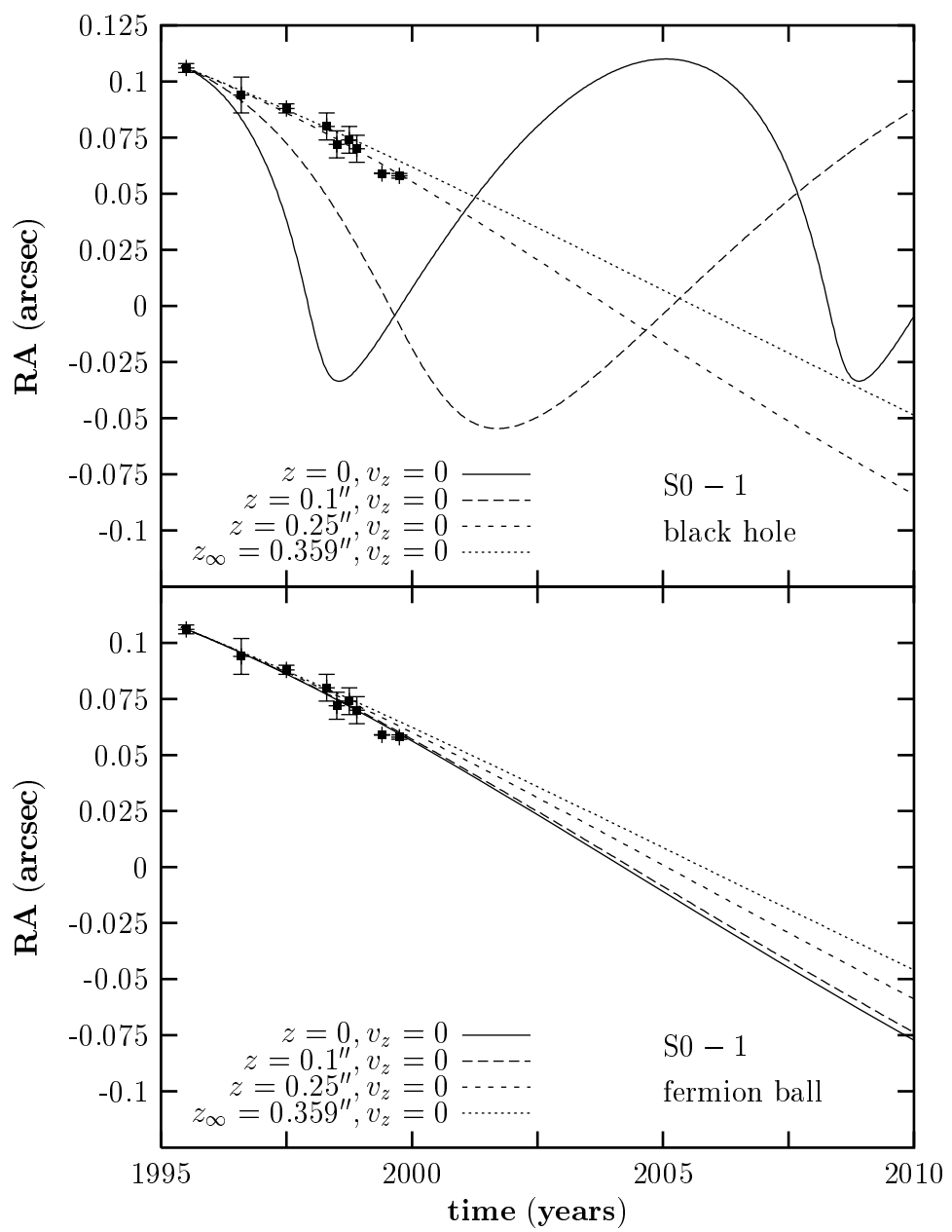


Fig.3

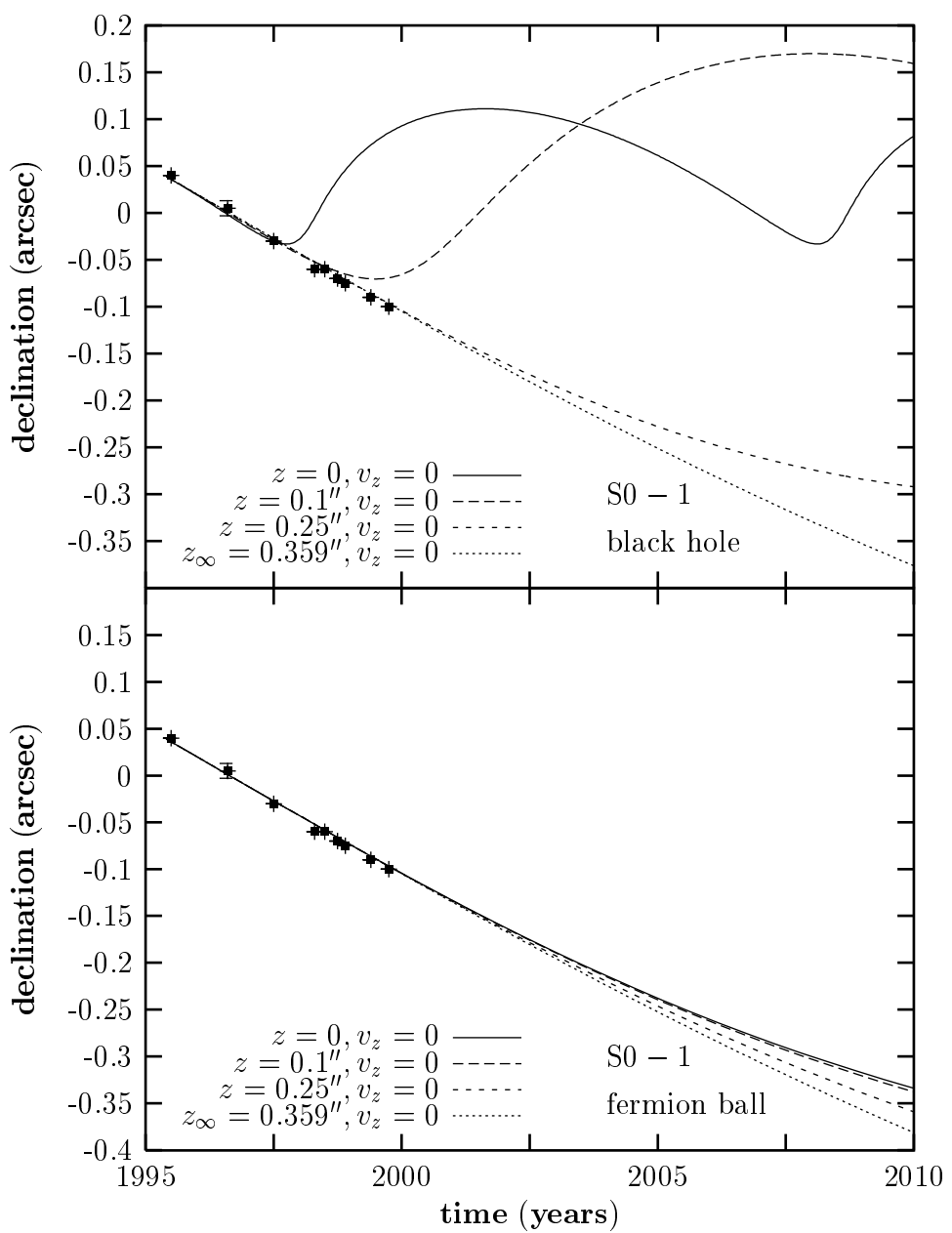


Fig.4

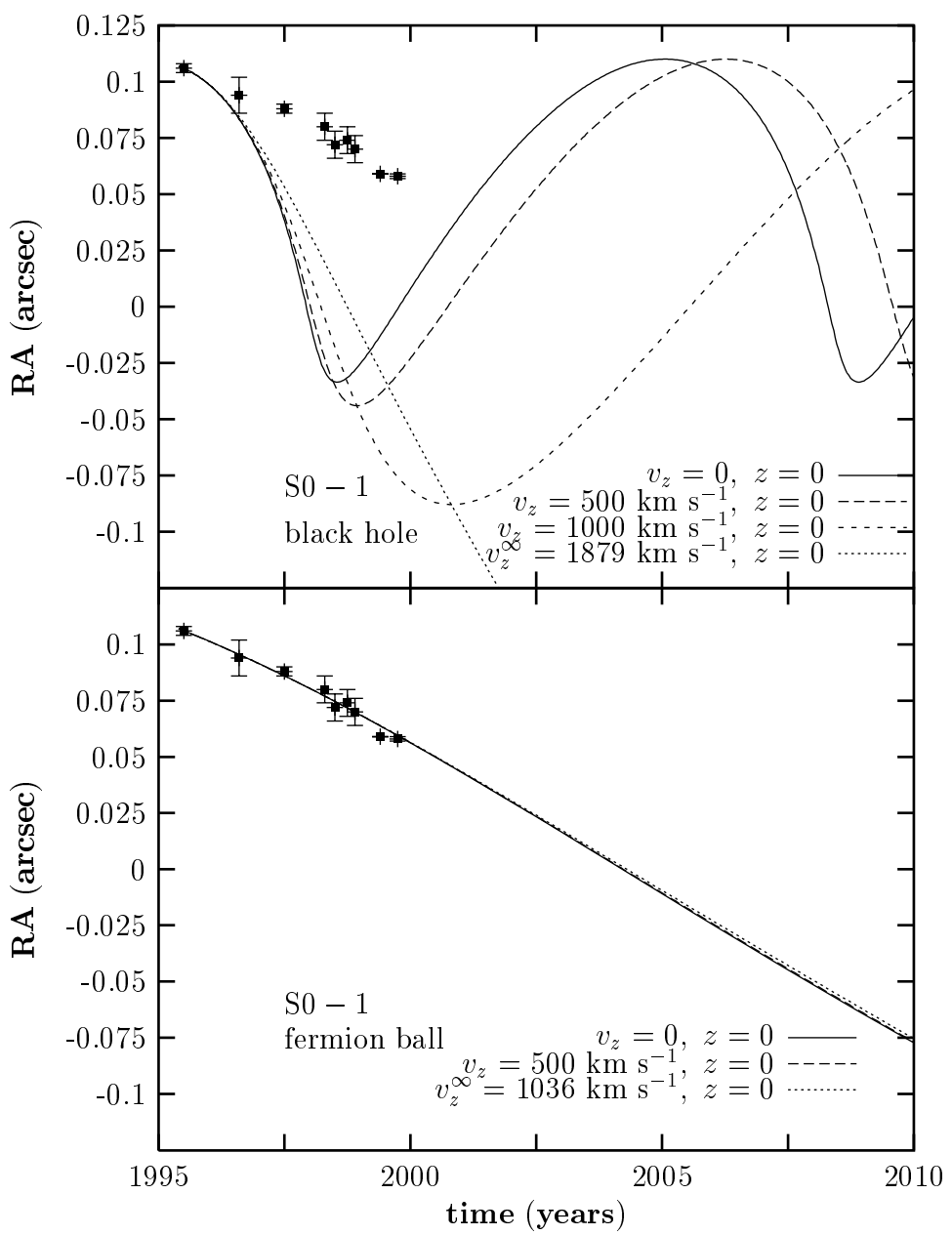


Fig.5

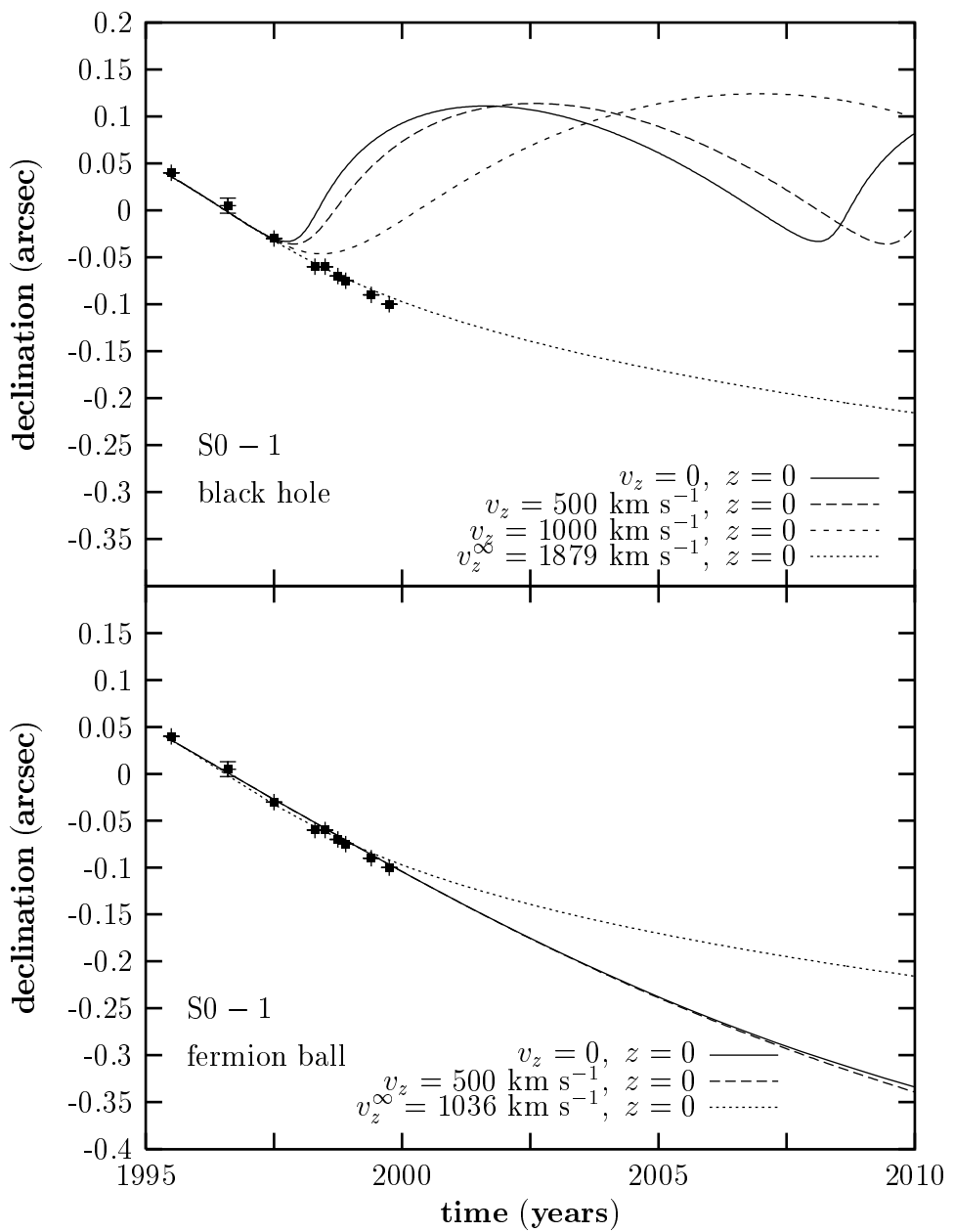


Fig.6

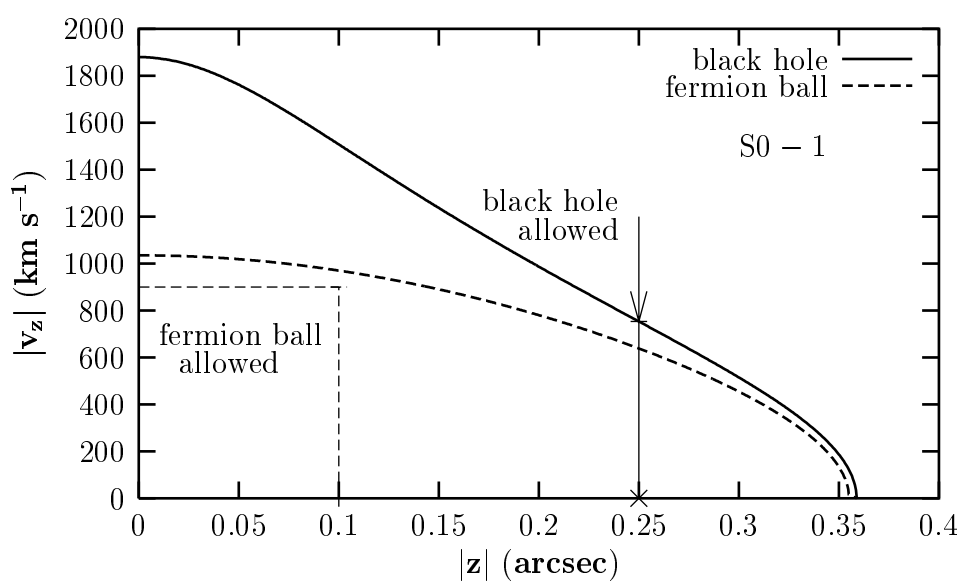


Fig.7

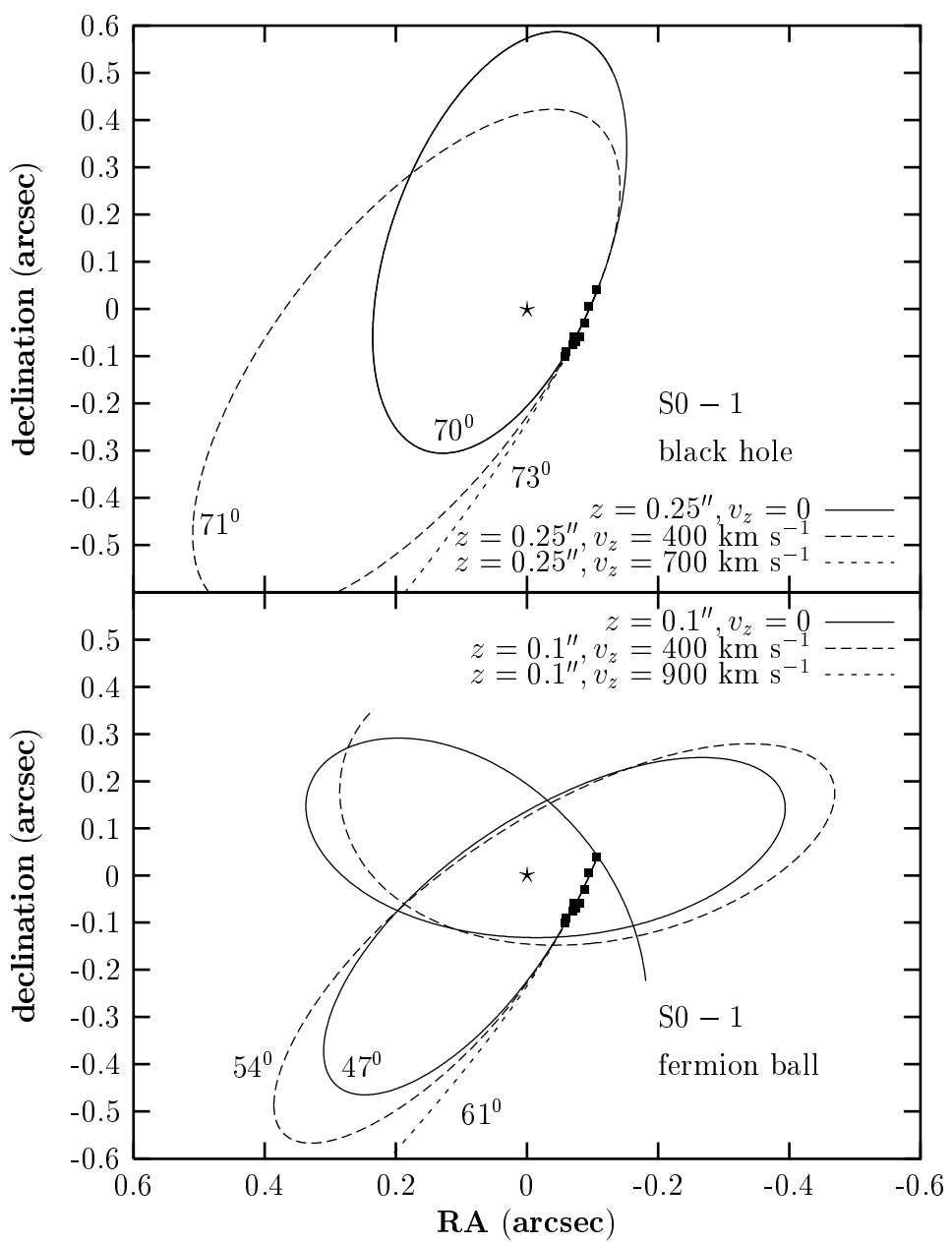


Fig.8

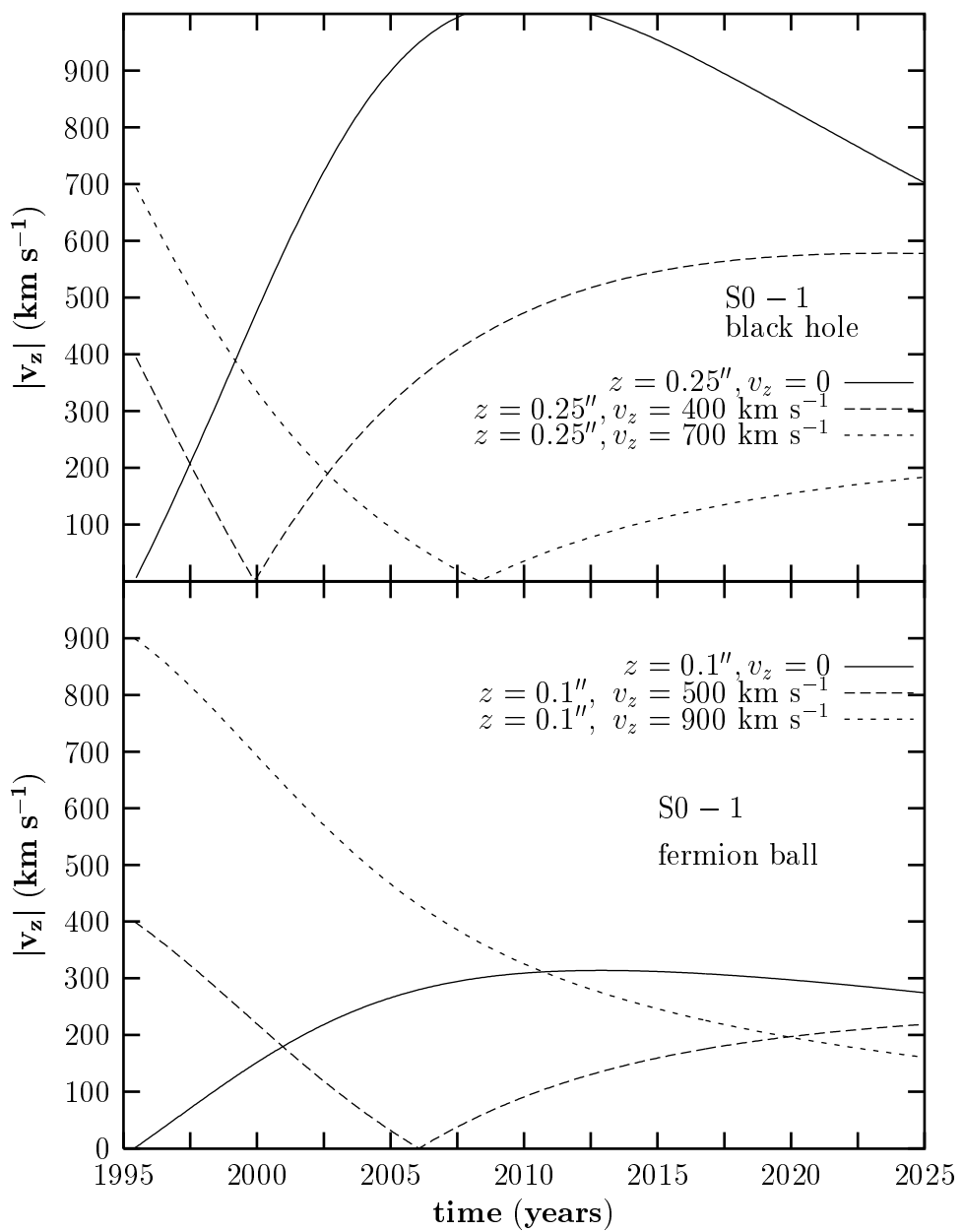


Fig.9

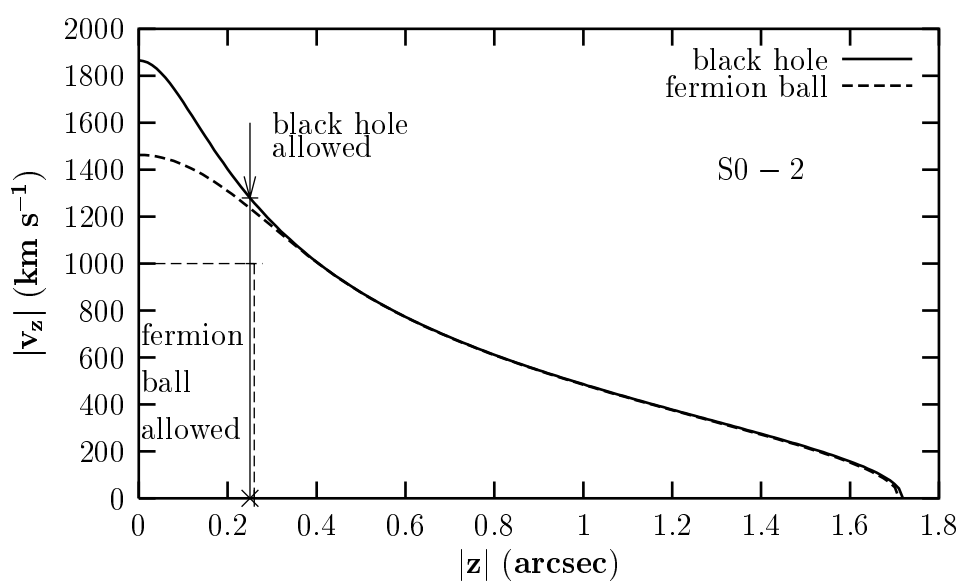


Fig.10

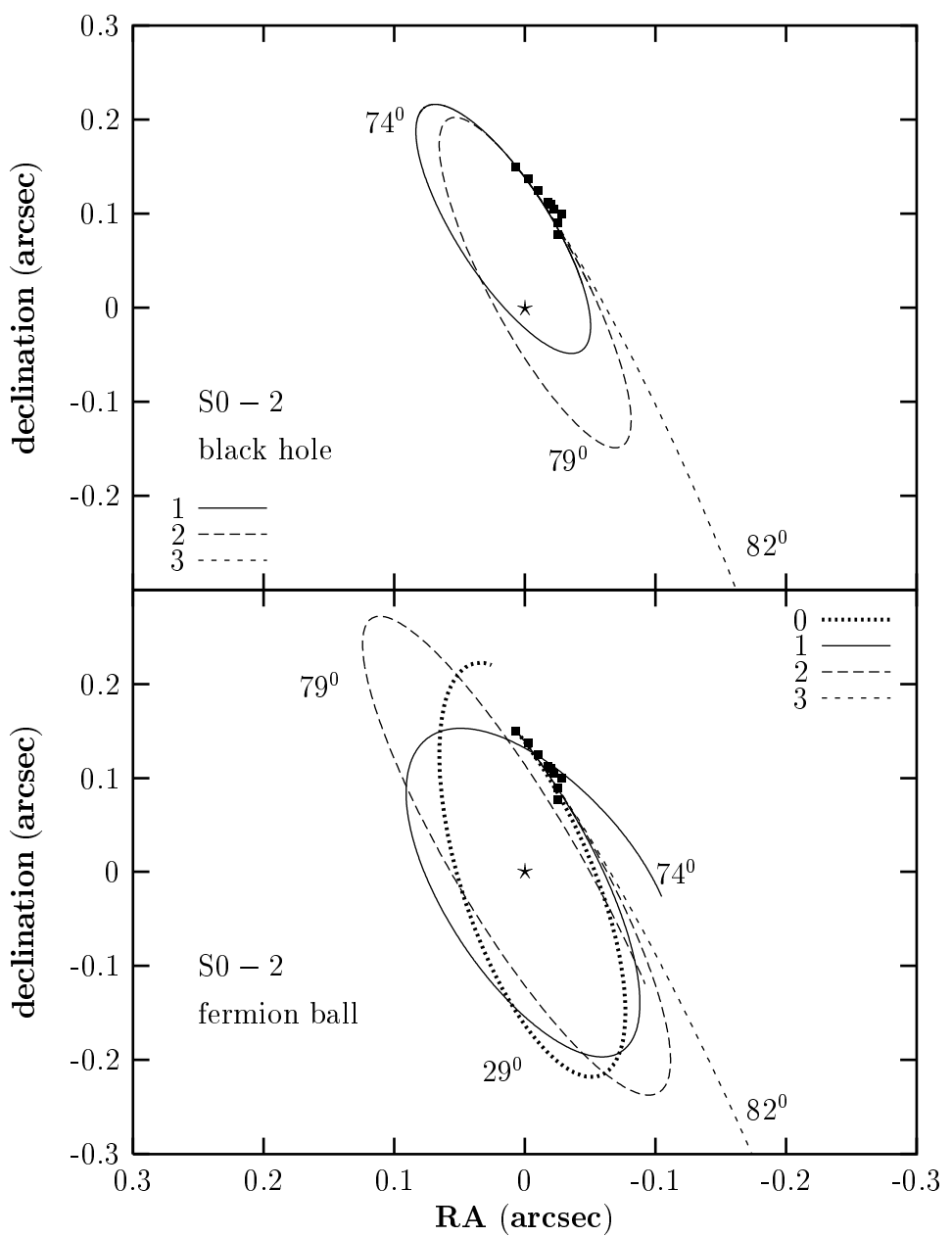


Fig.11

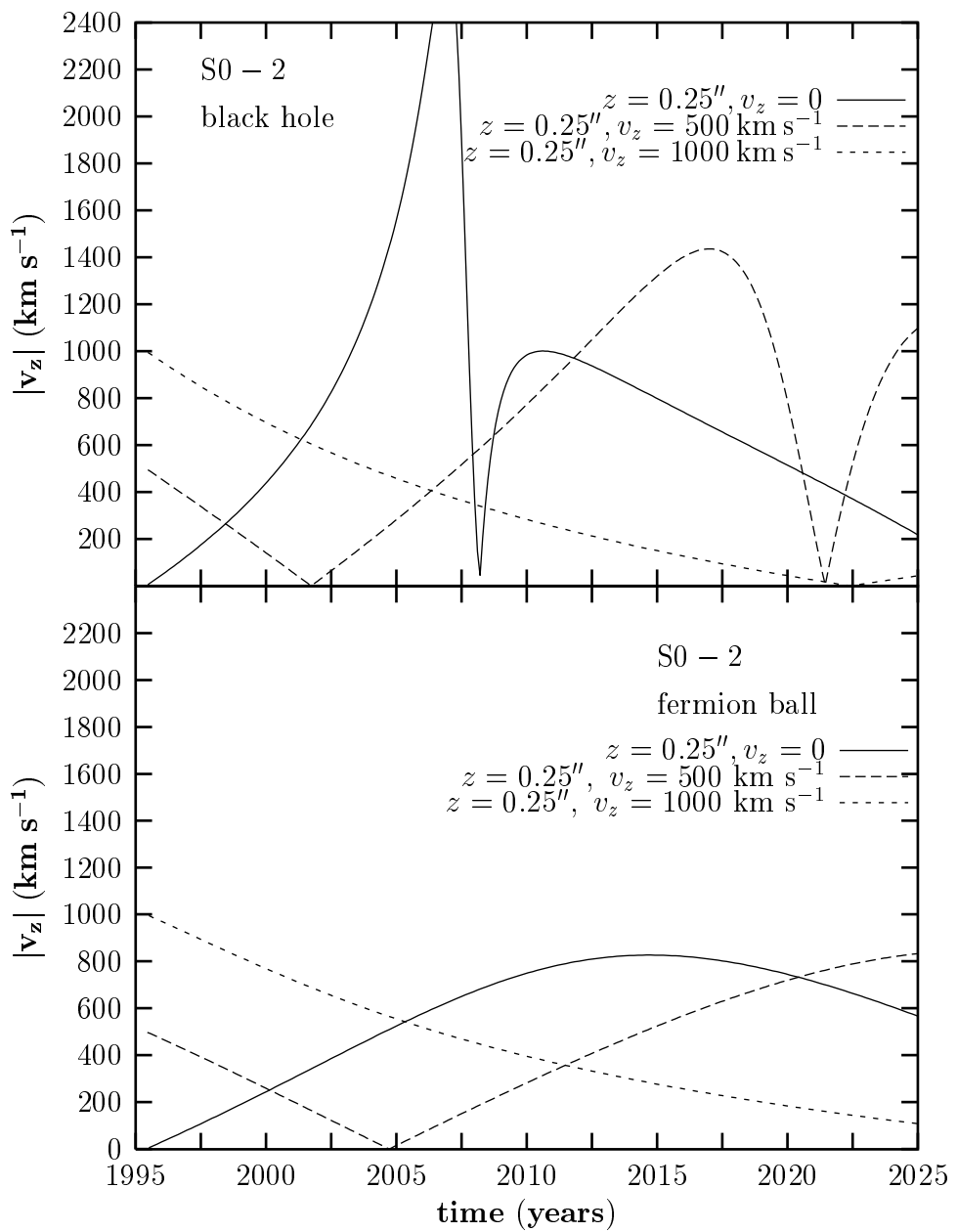


Fig.12